Supplementary Material (ESI) for Chemical Communications

Atomic-scale mechanistic features of oxide ion conduction in apatite-type germanates

Electronic Supplementary Material

1. Conductivity data for $La_{9.33}(GeO_4)_6O_2$

Experimental

Single phase $La_{9.33}(GeO_4)_6O_2$ was prepared via a Pechini-type sol gel route. Stoichiometric amounts of $La(NO_3)_3.9H_2O$ and GeO_2 were dissolved by heating in water. Once dissolved, citric acid and ethylene glycol were added (1.75 moles per mole of La), and the mixture evaporated on a hot plate until a clear gel was obtained. The gel was then transferred to a furnace and heated at 2°C/min to 800°C before holding at this temperature for 12 hours. Pellets (1.6 cm diameter) for conductivity measurements were prepared as follows: the powders were ball milled (350 rpm, Fritsch Pulverisette 7 Planetary Mill) for 1 hour before pressing at 8000 kg cm^{-2}. The pressed pellets were then heated at 1300°C for 2 hours, leading to a density of 91% theoretical. Both sides of the pellet were coated with Au paste and then heated to 700°C for 1 hour to ensure bonding to the pellet. Conductivity measurements were made in air using AC impedance spectroscopy (Hewlett Packard 4182A impedance analyser). Phase purity was confirmed through X-ray powder diffraction (Panalytical X'Pert Pro diffractometer, Cu $K\alpha_1$ radiation).

Figure 1 Conductivity data for $La_{9.33}(GeO_4)_6O_2$

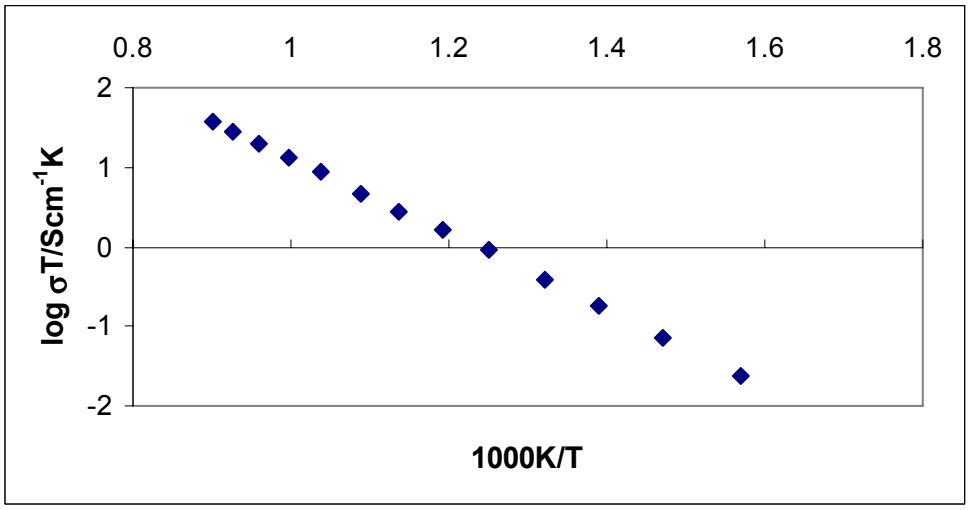

2. Interatomic potentials, comparison between calculated and experimental structures, and defect energies

Table 1. Interatomic potentials employed in the modelling studies

Buckingham	A (eV)	C (eV Å^{-6})	ρ (Å)	Y	K(eV Å^{-2})
Ge core O shell	1497.3996	0.325646	16.00	4.00	
La core O shell	4579.23	0.30437	0.00	3.00	
O shell O shell	22764.0	0.1490	27.879	-2.89	74.92

Table 2a. Comparison between experimental and calculated structures for $La_{9.33}(GeO_4)_6O_2$

	experimental	calculated	difference
a (Å)	9.9117	9.996269	0.85 %
b (Å)	9.9117	9.996269	0.84 %
c (Å)	7.2833	7.138881	-1.98 %
Vol (Å^3)	619.66	617.784	-0.3 %

Table 2b. Comparison between calculated and experimental bond distances for $La_{9.33}(GeO_4)_6O_2$

Bond		Experimental (Å)	Calculated (Å)	Difference (Å)
La1	O1	2.7862	2.8039	0.0177
	O2	2.5179	2.4984	-0.0195
	O3 x2	2.4504	2.4149	-0.0355
	O3 x2	2.6342	2.5966	-0.0376
	O4	2.3395	2.3654	0.0259
La2	O1 x3	2.4712	2.4573	-0.0139
	O2 x3	2.5821	2.5894	0.0073
	O3 x3	2.9132	2.9529	0.0397
Ge	O1	1.7348	1.7207	-0.0141
	O2	1.7264	1.7425	0.0161
	O3 x2	1.7348	1.7391	0.0043

Table 3. Frenkel and Schottky defect energies for $La_{9.33}(GeO_4)_6O_2$

Frenkel Defect	Total Energy (eV)	Energy per defect (eV)
O	2.94	1.47
Ge	23.28	11.64
La1	14.65	7.32
La2	7.70	3.85
Schottky Defect	Total Energy (eV)	Energy per defect (eV)
$La_{9.33}(GeO_4)_6O_2$	180.51	5.76
La_2O_3-type	21.28	4.26
GeO_2-type	14.74	4.91

3. Molecular dynamics (MD) results

The results showed that all the oxide ions are mobile, with the average activation energy in the range 873-1273K being 0.98 eV, which reduces to 0.61 eV at higher temperatures.

Figure 3. Diffusion coefficients for oxide ions from MD calculations

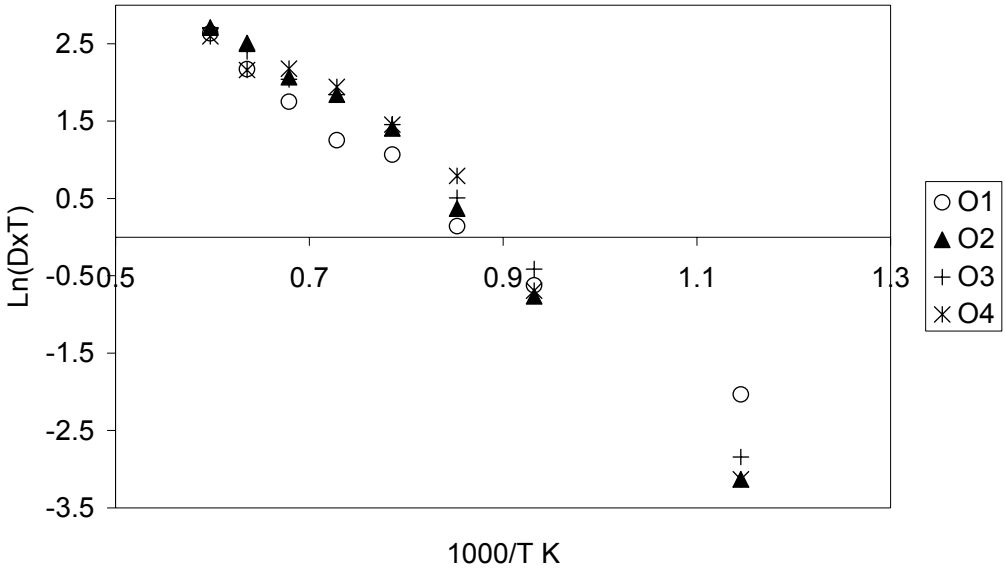

Figure 4. Snapshot of the oxygen trajectories from MD simulations at 1473K showing the "fan-like" conduction pathway along the c-axis between neighbouring GeO_4 units. The figure shows significant lattice relaxation during the conduction process.

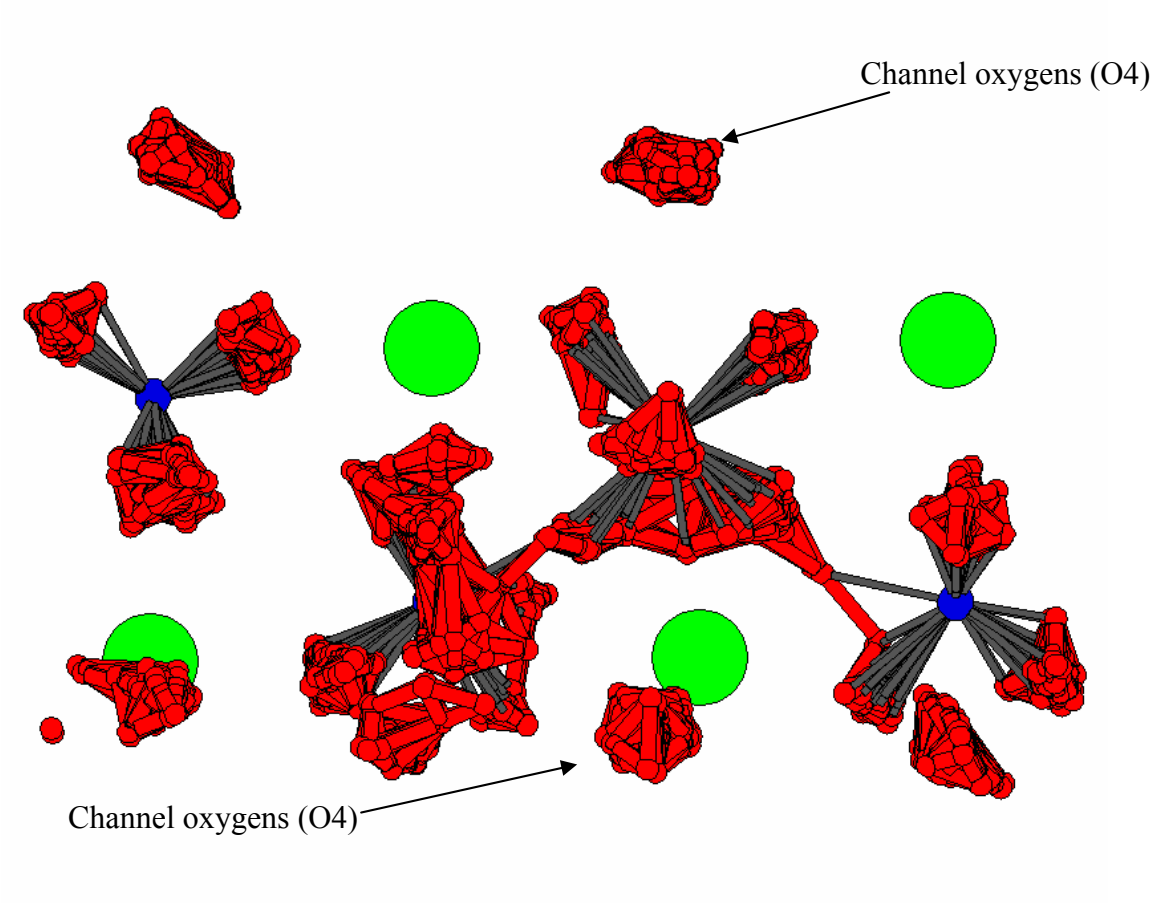

Figure 5. MD trajectory plot for oxygen diffusion at 1473K showing formation of interstitial defects and considerable motion of oxygens in the ab plane (red=O, white=Ge, Green=La)

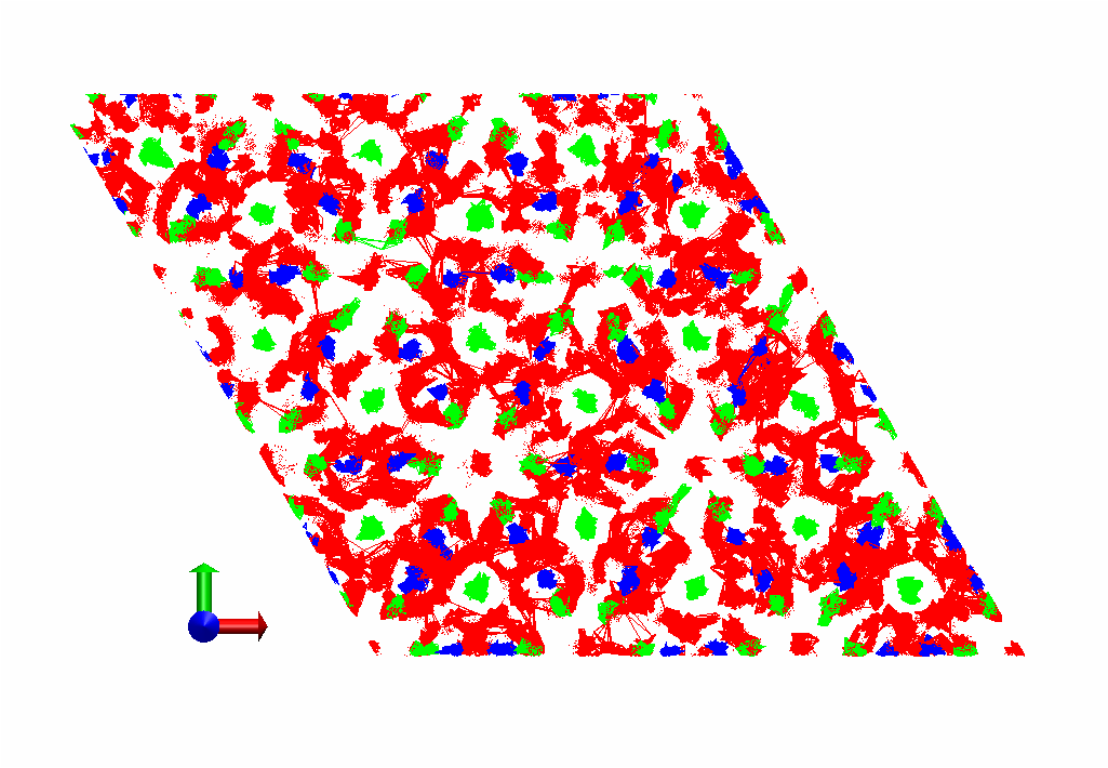

Figure 6. Skeletal drawings of the GeO_4 tetrahedra in $La_{9.33}(GeO_4)_6O_2$ at 1473K, showing a large degree of GeO_4 tetrahedra rotation